Proceedings of the 5th International Conference on Fluid Flow and Thermal Science (ICFFTS 2024)
Lisbon, Portugal- November 21 - 23, 2024
Paper No. 155
DOI: 10.11159/icffts24.155

Experimental Analysis Of A Newly Developed "Dado Cut" Square Pin-Fin Heat Sink For Avionics Cooling

Mayank Maroliya[1], Sandip K. Saha[2],
[1]Thermal Science Lab, Mechanical Engineering Department, IIT Bombay,
Powai, Mumbai, India, 400076.
214100015@iitb.ac.in; sandip.saha@iitb.ac.in
[1]Thermal Science Lab, Mechanical Engineering Department, IIT Bombay,
Powai, Mumbai, India, 400076.

Abstract **-** The increasing heat dissipation in modern electronic packages has necessitated the development of efficient and robust thermal management (TM) systems to ensure reliable operation. This study investigates the heat transfer performance of a newly designed 'dado cut' square pin fin (SPF) heatsink (or grooved square pin fin heatsink) integrated with a solid-solid phase change material (SSPCM) for passive cooling of avionics systems. The proposed heatsink design is experimentally evaluated and compared with a conventional SPF heat sink to quantify the enhancement in heat transfer. The experiments are conducted at various heat inputs (7 W, 11 W, and 13 W) and critical set point temperatures (SPTs). The effect of phase change material (PCM) volume fraction on the thermal performance of the SPF heat sink is also investigated. A 3.33% increase in exposed surface area and a reduction of 12.87% in weight are found with the dado-cut SPF heatsink design. The results demonstrate a significant improvement of 40.34% in safe operational time (SOT) by grooved SPF heatsink, thereby establishing the reliability of the avionics TM system. The findings of this study contribute to the development of efficient and compact thermal management solutions for avionics systems, which is crucial for ensuring the reliability and performance of modern electronic packages.

Keywords**:** Solid-Solid Phase Change Material, Avionics Cooling, Dado-cut Square Pin Fin Heatsink, Set Point Temperature, Safe Operational Time.

1. Introduction

The rapid advancements in the miniaturization and functionality of modern electronic devices have resulted in a significant increase in power densities, posing a critical challenge for thermal management [1]. Conventional cooling methods, such as natural, mixed, and forced convection, have proven inadequate in dissipating the heat generated by modern electronic components in such demanding environments. To address these thermal challenges in avionics, researchers have explored various active and passive cooling techniques [2]. These include molecular cooling fans utilizing nanomaterials [3], loop and hybrid heat pipes [4-7], thermoelectric coolers [8, 9], radiant heat sinks with fins [10], liquid cooling systems [11, 12], and vapor cycle systems [13]. While these approaches offer promising solutions, the stringent requirements of aircraft environments, such as lightweight design and rapid thermal response, necessitate alternative strategies.

Phase change material (PCM)-based Thermal Energy Storage (TES) has emerged as an efficient thermal management solution due to its ability to regulate thermal loads, high energy storage density, and substantial energy absorption and release during phase transitions. Recently, researchers have shown significant interest in solid-solid PCMs (SSPCMs). M. Maroliya et al. [14] compared SSPCMs and solid-liquid PCMs (SLPCMs) with similar phase transition temperatures in avionics applications. Results revealed that SSPCMs outperform SLPCMs in avionics due to superior stability and resistance to environmental factors, making them suitable for aerospace applications. Heat sinks are vital for ensuring the longevity of high-heat-generating electronic components. Research indicates that a larger surface area significantly enhances heat transfer compared to the height of the dissipation surface [15]. Despite advancements, the need for innovative thermal management solutions remains critical [16]. Traditional heat sinks, such as plate-fin and pin fin (circular, cylindrical, and rectangular-shaped) configurations, have been extensively studied and optimized to improve heat transfer performance. Standard optimization methods include adjustments to the number, shape, and arrangement of fins (in-line vs. staggered), utilization of fins with varying heights and aspect ratios, and incorporation of diverse perforation patterns on the fin surface.

Perforations, or strategically placed holes within the fin structure, reduce weight while increasing surface area. Perforations offer numerous benefits, including reduced overall heat sink weight, enhanced heat dissipation capacity, generation of vortices through the perforation area, and minimized pressure drop compared to non-perforated surfaces, leading to a more economical design. Wang and Charles [17] investigated the performance of rectangular, trapezoidal, and inverted trapezoidal configurations of heat sinks at heat loads ranging from 3 W to 20 W. Cyril et al. [18] explored the influence of different fin configurations (square, circular, triangular, tapered square, tapered circle, tapered triangle) with varying fin and base thicknesses and numbers of fins on SSPCM-based thermal control modules for avionics applications. Their results indicated that triangular fins performed significantly better, with 25% and 35% weight reductions compared to square and circular counterparts, respectively. Sparrow, Ramsey, and Altemani [19] demonstrated that in-line array fins exhibit significantly lower heat transfer performance compared to staggered-arranged fins.

Several investigators have also explored the possibility of perforated heat sinks. A study by Chin et al. [20] demonstrated that perforations enhance convection heat transfer by 45% compared to solid pins. Gupta, Saha, and Roy [21] found that the performance of fins with up to three perforations was superior to that of solid square micro fins. Li, Jeon, and Byon [22] conducted a numerical investigation comparing the performance of perforated radial heat sinks to non-perforated ones, highlighting the enhanced thermal management capabilities of perforated designs. Shaeri and Yaghoubi [23] conducted a numerical analysis of turbulent convective heat transfer in solid and perforated fin arrays. Their findings indicated that longitudinal perforations significantly enhance heat transfer compared to solid fins. Additionally, the perforations reduced the weight of the heat sink by 37% while improving heat transfer efficiency. Furthermore, Xie et al. [24] studied the numerical model of a PCM-based heat sink with various tree-shaped structures, including topology optimization. Their findings indicated that these innovative designs achieved higher efficiency than conventional heat sinks.

Despite extensive research on conventional and perforated pin fin heat sinks to improve thermal performance, finding efficient passive cooling solutions for high-power electronic components remains a significant challenge. This study introduces a novel heat sink design that incorporates 'dado cut' SPF fins integrated with solid-solid phase change material (SSPCM). The primary goal is to experimentally evaluate the thermal performance of this innovative design compared to a conventional solid SPF heat sink. A comprehensive experimental setup was developed to conduct tests under varying heat loads and PCM volume fractions, assessing key performance metrics such as weight, safe operating time, set point temperature, and enhancement ratio through parametric analysis. A thorough literature review identified a notable gap in research on the heat transfer characteristics of 'dado cut' or laterally grooved SPF fin heat sinks integrated with SSPCMs for passive cooling. This pioneering study explores the potential benefits of the novel design, which is expected to reduce weight while maintaining or improving heat transfer efficiency.

2. Experimental Methodology

2.1. Experimental Setup

This study experimentally investigates the transient thermal performance of an innovative "dado cut" square pin fin (SPF) heat sink embedded with a solid-solid phase change material (SPCM) for thermal management in avionics applications. The heat sink, featuring slotted SPF, was fabricated using wire-cut electric discharge machining (EDM), tailored to specific dimensional and material requirements. Figure 1 presents a schematic overview of the experimental setup, highlighting an expanded view of the heat sink assembly. The primary components of this apparatus includes a Regulated DC power supply, a Data Logger, K-type thermocouples, a Laptop, and the Heatsink assembly itself. A constant input heat flux of 7 W, 11 W, and 13 W was provided by the regulated DC power supply (Aplab LQ6324T, 32V/2A), in alignment with typical power densities of electronic components. The digital data acquisition system (Keithley 2700 Multimeter/Data Acquisition System), connected to the thermocouples, was interfaced with the laptop. The temperature data was recorded at 10-second intervals using Keithley Kickstart ver. 2.11.1 software throughout the experiment. The selected ‘X55’ SSPCM (PCM Products Ltd., U.K.) has a phase transition temperature range of 51-72 °C, which aligns with the operational temperature range expected for electronic modules in aircraft avionics. All experiments were conducted at an initial temperature of 20 °C within a controlled environment, with the properties of the SSPCM detailed in Table 1.

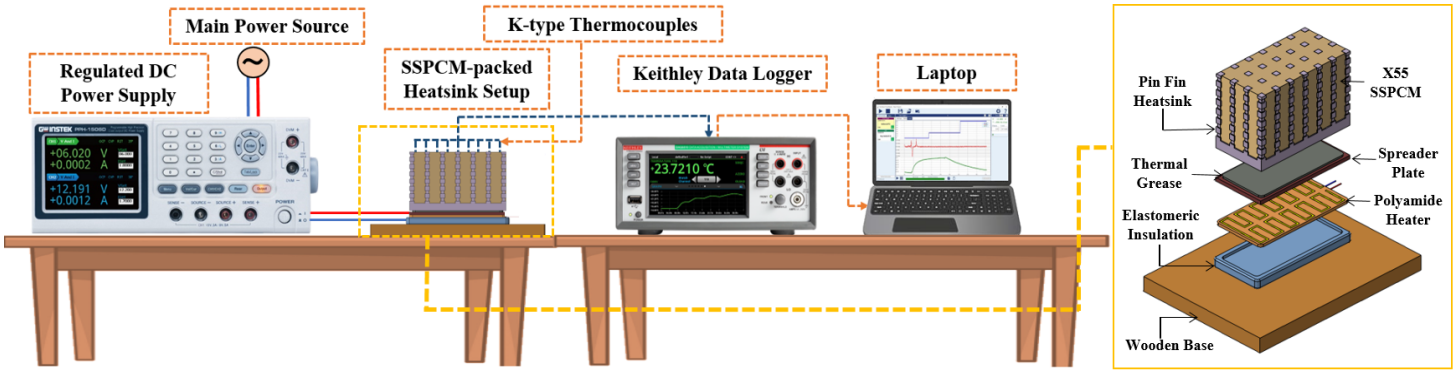

Fig. 1: Schematic of Experimental Setup with heatsink assembly

Table 1: Thermophysical Properties of SSPCM and Heatsink.

Material	ρ [kg/m^3]	T_t[°C]	C_p [J/kg-K]	k [W/m-K]	Ref.
X55	1060	51-72	1620	0.36	[25]
Al 6061 Heatsink	2712.9	-	960	179.6	[26]

2.2. Heatsink Assembly

This experimental study explores the thermal performance of a "dado cut" square pin fin (SPF) heat sink filled with solid-solid phase change material (SSPCM) and compares it to a solid SPF heat sink. The heat sink, constructed from aluminium alloy with dimensions of 61 mm x 31 mm x 5 mm, (side = 3 mm, height = 35 mm), chosen to be compatible with electronic packages. Grooves of 3 mm length and 2 mm depth were machined into the fins at a 3 mm pitch, maintaining a TCE% of 8-10% [26,27] while preserving structural integrity and manufacturability. As illustrated in Figure 1, a wooden base was selected for its excellent structural strength and thermal insulation properties. A flexible polyimide film heater (Omega Engineering, USA) is employed as the heat source, with its base insulated using a thin elastomeric rubber sheet (Supreme Industries Ltd., Mumbai) to minimize heat loss. A heat spreader plate is positioned above the heater to ensure even heat distribution and promote effective heat transfer. The generated heat is then conducted to the SSPCM-filled “dado cut” SPF heat sink mounted atop the spreader plate. To further enhance heat transfer and reduce thermal contact resistance, thermal grease (Perfect Solutions, India) is applied between the spreader plate and the heat sink.

Fig. 2: (a) Solid and Grooved SPF Heatsinks (b) Experimental Arrangement

2.3. Locations of Thermocouple

Figure 2 illustrates the placement of thermocouples within the heat sink, providing a detailed view of their strategic positioning to monitor the SSPCM's phase transition characteristics. Twelve K-type thermocouples (TC Direct, U.K., 0.2 mm diameter) are used: one (T0) at the bottom to measure heater temperature, four (T1-T4) at the base to detect temperature variations, and four (T5-T8) at the fins' top to observe ambient temperature and natural convection effects. Additionally,

three thermocouples (T9-T11) are vertically embedded in the honeycomb heat sink at 5 mm, 10 mm, and 15 mm intervals from the base to record temperature profiles within the core. Araldite™ epoxy resin secures the thermocouples for precise measurements. Thermocouples were calibrated in a water bath (Julabo FP51-SL Refrigerated Circulator) over 20-95 °C, ensuring consistency with a reference mercury thermometer.

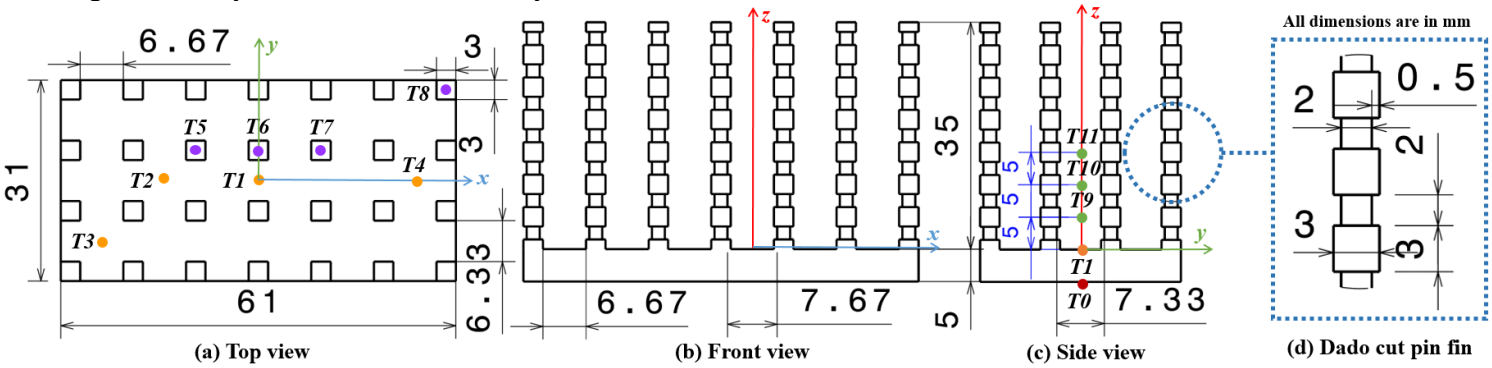

Fig. 3: Geometric Domain and Location of Thermocouples for the 'dado cut' SPF heat sink

Table 2: Boundary Conditions

Boundary Conditions	Case#1	Case#2	Case#3
	Heat Input		
1. Charging cycle (0<t ≤900 s)	q = 7 w	q = 11 w	q = 13 w
2. Discharging cycle (900 s<t ≤5100 s)	q = 0 w	q = 0 w	q = 0 w
3. Sidewall convective heat transfer	$-k_{al}\frac{\partial T}{\partial x}\Big\|_{x=0,L} = h_s\left(T\Big\|_{x=0,L} - T_{amb}\right)$		
4. Top wall convective heat transfer	$-k_{al}\frac{\partial T}{\partial y}\Big\|_{y=H} = h_t\left(T\Big\|_{y=H} - T_{amb}\right)$		

2.4. Input parameters, Boundary conditions and Uncertainty analysis

The experiment was performed for three different cases, i.e., Case #1, Case #2, and Case #3, with a heat load of 7 W, 11 W, and 13 W, respectively, for a charging cycle of 900 s. The boundary conditions are listed in Table 2. The initial temperature *(T_i)* and surrounding temperature *(T_{surr})* of 20 °C were considered for the entire experiment. The transient thermal characteristics of individual heat input cases were analyzed by examining variations in temperature for the duty cycle, monitored by the thermocouples, recorded by the data logger, and stored by the computer at regular intervals. The outcomes obtained from the experiments were plotted and compared against the experimental findings for a solid SPF heat sink. A non-dimensional parameter defined as the ratio of safe operational time with PCM to safe operational time without PCM, known as Enhancement Ratio (ε) [14], is utilized for parametric study. Mathematically, it is expressed as shown in Eq.1,

$$\varepsilon = \frac{SPT_{with\ SSPCM}}{SPT_{without\ SSPCM}} \tag{1}$$

The primary sources of experimental uncertainty originated from temperature measurements acquired using K-type thermocouples (TCN Direct, UK) with a stated accuracy of ± 0.5 °C within the 0-200 °C range. Electrical current and voltage, respectively measured by an ammeter (±0.1% uncertainty) and a voltmeter (±0.01% uncertainty), were combined to determine heater power. The Keithley 2700 Data Acquisition system introduced an additional uncertainty of ± 0.05 °C. It is important to note that the overall uncertainty in heater power calculation, derived from the product of voltage and current, was propagated according to Equation 2.

$$P = VI \tag{2}$$

$$\delta P = \sqrt{\left(\frac{\partial P}{\partial I}\delta I\right)^2 + \left(\frac{\partial P}{\partial V}\delta V\right)^2} = \sqrt{(V\delta I)^2 + (I\delta V)^2} \tag{3}$$

A sample calculation for a 32 V, 2 A system (64 W) yielded an approximate power uncertainty of ±0.06432 W, as detailed in Equation 3.

3. Result

3.1. Comparison of 'dado cut' vs solid SPF heatsink

This section discusses the comparison between the 'dado-cut' SPF heatsink and the solid SPF heatsink. Physically, the dado-cut SPF heatsink exhibits a 12.87% reduction in weight and a 3.33% increase in contact surface area. Figures 4a-4d show the heater temperature variations for both designs across different PCM volume fractions with a constant heat input rate. The base temperature, recorded by Thermocouple T0, was used to plot the temperature effects. For a consistent heat flux of 7 W and 11 W, the 'dado-cut' SPF heatsink demonstrated a notable temperature difference compared to the solid SPF heatsink across all PCM volume fractions. At a 7 W heat input, temperature differences of 3.56 °C, 2.58 °C, 2.51 °C, and 2.39 °C were observed between the two heatsink configurations for $\Psi = 0.0$, $\Psi = 0.33$, $\Psi = 0.66$, and $\Psi = 0.99$, respectively, at the end of the charging cycle. A similar trend was observed at the 11 W heat input. The 'dado-cut' SPF heatsink achieves better heat dissipation due to its increased surface area, resulting in more efficient heat transfer. At $\Psi = 0.0$, the largest temperature difference was observed, attributed to the cuts in the pin fins, which induce turbulence in the airflow around the grooved fins, thereby enhancing convective heat transfer. Consequently, the grooved fins provide superior thermal performance in managing avionics' thermal loads.

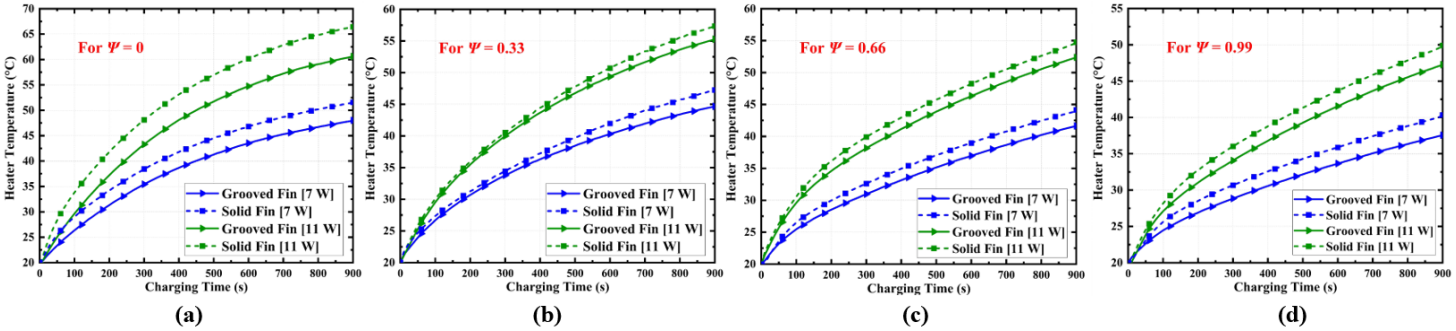

Fig. 4: Schematic of Experimental Setup with heatsink assembly

3.2. Effect of PCM volume

To evaluate the impact of SSPCM volume on the thermal performance of heat sinks, four distinct volumetric ratios ($\Psi = 0.0$, $\Psi = 0.33$, $\Psi = 0.66$, $\Psi = 0.99$) were selected. Each heat sink configuration was subjected to a constant heat load of 13 W, as depicted in Figure 5(a). The results revealed consistent trends across all heat sink configurations for each PCM volumetric fraction. At $\Psi = 0.0$, a rapid rise in base temperature was observed, attributed to the absence of PCM within the heat sink. Conversely, when the heat sink was partially filled with PCM in three equal fractions, there was a marked improvement in thermal performance, particularly in extending the latent heat phase for the 'dado-cut' SPF heat sink configuration. The end temperature values recorded were 75.6 °C, 60.1 °C, 57.5 °C, and 54.1 °C for $\Psi = 0.0$, $\Psi = 0.33$, $\Psi = 0.66$, and $\Psi = 0.99$, respectively. These findings highlight that a heat sink with a volumetric fraction of $\Psi = 0.99$ offers substantial benefits for the thermal management of electronic devices.

3.3. Effect of heat input

To assess the impact of varying heat fluxes on the thermal behavior of a 'dado-cut' SPF heatsink filled to a volumetric fraction of $\Psi = 0.99$ with SSPCM, three heat input levels, i.e.,7 W, 11 W, and 13 W were examined, as illustrated in Figure 5(b). The average temperature distribution of the SSPCM was recorded using thermocouples T9-T11, strategically placed to provide a representative thermal profile. The average SSPCM temperatures measured at the end of the charging cycle were 35.8 °C for 7 W, 45.7 °C for 11 W, and 51.6 °C for 13 W. These results indicate that higher heat flux results in a more pronounced temperature rise in the SSPCM during the sensible heating phase. Notably, at heat fluxes of 7 W and 11 W, no phase change was detected within the PCM, even after 900 seconds of heating. However, a phase transition was observed at the higher heat input of 13 W, commencing after approximately 694 seconds. The phase transition behavior of the SSPCM under higher heat flux conditions enables effective absorption of heat, thereby moderating the temperature rise and potentially extending the operational life of the electronic components by improving thermal management efficiency.

3.4. Set Point Temperature (SPT) and Enhancement Ratio (ε) analysis

Thermal performance in terms of set point temperatures (SPT) for a heat flux of 7 W, 11 W, and 13 W, respectively, is shown in Table 3. The temperature of 40 °C is chosen as critical SPT. Table 3 shows that the time taken to reach SPT is longer for solid SPF heatsinks than for 'dado-cut' SPF heatsink configurations for all heat input-PCM volume combinations. Figure 5(c) reflect the enhancement ratio (ε) for SPTs of 40 °C against various input heat fluxes for both configurations of PCM filled heat sinks at various Ψ. The maximum value of ε, recorded for a solid SPF heat sink and 'dado-cut' SPF heatsink, was 2.56 and 2.88, respectively, at an input heat input of 13 W. It is found that for a case with q = 7 W and $\Psi = 0.99$ (see Figure 5(c)), the heater temperature is always below the SPT during the entire charging, making it unconditionally safe to operate. With increased surface area and reduction in thermal resistance, the dado-cut SPF heatsink can effectively improve the operational life of electronics. When combined with SSPCM, the dado-cut SPF heatsink can more effectively manage and distribute the heat absorbed by the SSPCM. The grooves promote uniform heat distribution within the SSPCM, enabling it to absorb more heat and undergo phase transitions more efficiently. This improved thermal management delays the rise in temperature in the system, resulting in a longer SOT.

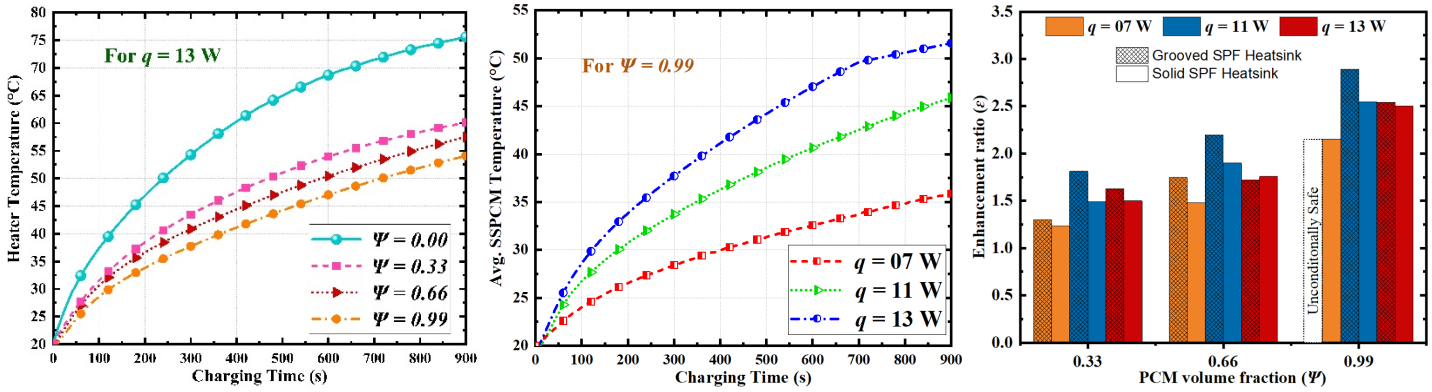

Fig. 5: (a) Heater temperature variation at different Ψ. (b) SSPCM temperature variation at different q. (c) Enhancement ratio for two heatsink configurations for different PCM volumes and heat input

Table 3: Safe Operational Time (SOT) for a Set Point Temperature (SPT) = 40 °C.

Dado-cut SPF Heatsink				**Solid SPF Heatsink**			
PCM-volume	**q = 7 w**	**q = 11 w**	**q = 13 w**	**PCM-volume**	**q = 7 w**	**q = 11 w**	**q = 13 w**
$\Psi = 0.00$	452 s	247 s	127 s	**$\Psi = 0.00$**	347 s	176 s	164 s
$\Psi = 0.33$	588 s	304 s	230 s	**$\Psi = 0.33$**	518 s	286 s	246 s
$\Psi = 0.66$	789 s	365 s	279 s	**$\Psi = 0.66$**	659 s	303 s	288 s
$\Psi = 0.99$	-	531 s	367 s	**$\Psi = 0.99$**	884 s	447 s	420 s

4. Conclusion

A heat transfer enhancement by the dado-cut SPF heatsink is explored in this experimental research. Tests were conducted with three different heat inputs (7 W, 11 W, 13 W) and four different PCM volume fractions (0%, 33%, 66%, 99%) on a dado-cut SPF and conventional SPF heat sink. To investigate the effectiveness of grooved SPF, an SPT of 40 °C was selected, and SOT was explored. The following results were derived;

- The dado-cut SPF heatsink design resulted in a 3.33% increase in exposed surface area and a 12.87% reduction in weight compared to the conventional solid SPF heatsink.
- The maximum improvement in SOT for a dado-cut SPF heatsink compared to a solid SPF heatsink was found to be 40.34%, with an average improvement of 19.05%, revealing better heat transfer characteristics.
- It is concluded from the experimental examinations that, for a heatsink filled with SSPCM ($\Psi = 0.99$) under a heat load of 7 W, the electronics remained unconditionally safe to operate, consistently maintaining temperatures below the operational limit of 40 °C.
- The results indicate that the enhancement ratio (ε) increases with higher SSPCM volumes and lower heat input rates. The maximum enhancement ratio (ε) improvement observed was 25.1% for the configuration with $\Psi = 0.99$ and $q = 13$ W, highlighting the SSPCM's enhanced heat storage capacity at elevated heat loads.

Acknowledgments

The authors would like to acknowledge the fabrication and experimental facility provided by the EV Powertrain Lab, Department of Electrical Engineering, IIT Bombay, Mumbai. and Thermal Science Lab, Department of Mechanical Engineering, IIT Bombay, Mumbai. The authors also thankful for the financial support (EEQ/2021/000004) from the Department of Science and Technology, Government of India.

References

[1] S. Krishnan, "A novel hybrid heat sink using phase change materials for transient thermal management of electronics," in *Proceedings of the Intersociety Conference* 1, 2004, pp. 310–318.

[2] N. Ali, "Passive Thermal Management for Avionics in High Temperature Environment", University of Gujrat, Pakistan. [Online]. Available: https://www.slideshare.net/Hamayun14373Liaqat/passive-thermal-management-for-avionics-in-high-temperature-environment.

[3] Eyassu T., and Hsiao TJ, "Molecular cooling fan: factors for optimization of heat dissipation devices and applications," Industrial & Engineering Chemistry Research, vol. 53(50), 2014.

[4] Riehl R.R., and Dutra T., "Development of an experimental loop heat pipe for application in future space missions." *Appl. Therm. Eng.,* vol. 25, pp. 101-112, 2005.

[5] A. AlShehhi, and A. AlMarar, "Thermal design evaluation of loop heat pipe for small satellite applications using graphene Nano-Particles," in *70th International Astronautical Congress (IAC*), Washington D.C., U.S.A, 2019.

[6] T. Hoang, "Development of a two-phase capillary pumped heat transport for spacecraft central thermal bus," in *American Institute of Physics (AIP) Conference Proceedings*, vol. 654, 2003, pp. 49-54.

[7] J. Yun, D. Bugby, "Thermal performance of multi-evaporator hybrid loop heat pipe (ME-HLHP) with a liquid cooled shield (LCS)', in *5th International Energy Conversion Engineering Conference and Exhibit (IECEC)*, St. Louis, 2007.

[8] V.K. Singh, S.S. Sisodia, A. Patel, T. Shah, P. Das, R.N. Patel, and R.R. Bhavsar, "Thermoelectric cooler (TEC) based thermal control system for space applications: Numerical study," *App. Ther. Eng.*, vol. 224, 120101, 2023.

[9] Yan W. N. and K. H. H. Li, Application of ThermoElectric Cooler (TEC) in avionics for thermal management, in *IEEE/AIAA 34th Digital Avionics Systems Conference (DASC)*, Prague, Czech Republic, 2015, pp. 6D5-1-6D5-14.

[10] Yu Xu, Jiale Wang, Tong Li, "Experimental study on the heat transfer performance of a phase change performance of a phase change material based pin-fin heat sink for heat dissipation in airborne equipment under hypergravity," *J. of Energy Storage*, vol. 52A, 104742, 2022.

[11] R. LeVasseur, "Liquid-cooled approaches for high-density avionics," in *IEEE/AIAA 10th Digital Avionics Systems Conference*, Los Angeles, CA, USA, 1991, pp. 147-152.

[12] D. Pal and M. Severson, "Liquid-cooled system for aircraft power electronics cooling," in *16th IEEE Intersociety Conference on Thermal and Thermomechanical Phenomena in Electronic Systems (ITherm)*, USA, 2017, pp. 800-805.
[13] P.E. Phelan, V. Chiriac, T.Y.T. Lee, "Current and future miniature refrigeration cooling technologies for high power microelectronics," in *IEEE Transactions on Components and Packaging Technologies*, vol. 25, 2002, pp. 356-365.
[14] M. Maroliya, Midhun V.C., and S.K. Saha, "Evaluation of solid-solid and solid-liquid phase change materials in pin-finned heat sinks for cooling of avionics electronics," *Thermal Science and Eng. Progress,* vol. 53, 2024, 102781.
[15] K. Subahan, E. Siva Reddy, and R. M. Reddy, "CFD analysis of pin-fin heat sink used in electronic devices," *Int. J. Sci. Technol. Res*., vol. 8, pp. 562-569, 2019.
[16] H. Yin, X. Gao, J. Ding, and Z. Zhang, "Experimental research on heat transfer mechanism of heat sink with composite phase change materials," *Energy Convers. Management,* vol. 49(6), pp. 1740–1746, 2008.
[17] R. Charles, and C.C. Wang, "A novel heat dissipation fin design applicable for natural convection augmentation," *Int. Comm. of Heat and Mass Tran.,* vol. 59, pp. 24–29, 2014.
[18] C.R. Raj, S. Suresh, "Influence of fin configuration in the heat transfer effectiveness of Solid-Solid PCM based thermal control module for satellite avionics: Numerical simulations," *J. of Energy Storage*, vol. 29, 101332, 2020.
[19] E.M. Sparrow, J.W. Ramsey, and C.A.C. Altemani, "Experiments on in-line pin fin arrays and performance comparisons with staggered arrays*," J. Heat Tran*., vol.102, pp. 44–50, 1980.
[20] S.B. Chin, J.J. Foo, Y.L. Lai, and T.K. Yong, "Forced convective heat transfer enhancement with perforated pin fins," Heat *Mass Tran.*, vol. 49 (10), pp. 1447–1458, 2013.
[21] D. Gupta, P. Saha, and S. Roy "Numerical investigation on heat transfer enhancement with perforated square micro-pin fin heat sink for electronic cooling applications," in *IEEE 21st Electronics Packaging Technology Conference*, Singapore, 2019, pp. 241–246.
[22] B. Li, S. Jeon, and C. Byon, "Investigation of natural convection heat transfer around a radial heat sink with a perforated ring," *Int. J. Heat Mass Tran.*, vol. 97, pp. 705–711, 2016.
[23] M.R. Shaeri, and M. Yaghoubi, "Numerical analysis of turbulent convection heat transfer from an array of perforated fins," *Int. J. Heat Fluid Flow*, vol. 30 (2), pp. 218–228, 2009.
[24] J. Xie, K.F. Choo, J. Xiang, and H.M. Lee, "Characterization of natural convection in a PCM-based heat sink with novel conductive structures," *Int. Commun. Heat Mass Tran.*, vol. 108, 104306, 2019.
[25] "PlusICE Solid-Solid PCM," PCM Product Ltd., Cambridgeshire, United Kingdom. Available from: https://www.pcmproducts.net/files/PlusICE%20Range%202021-1.pdf.
[26] S.K. Saha, K. Srinivasan, and P. Dutta, "Studies on optimum distribution of fins inheat sinks filled with phase change materials," *J. Heat Transfer*, vol. 130 (3), pp. 034505-1-034505-4, 2008.
[27] R. Baby, and C. Balaji, "Thermal optimization of PCM based pin fin heat sinks: an experimental study," *Appl. Therm. Eng*., vol. 54 (1), pp. 65–77, 2013.